Practical Basis of the Geometric Mean Fitness and its Application to Risk-Spreading Behavior

Practical basis of the geometric mean fitness and its application to risk spreading behavior

Takuya Okabe[1] and Jin Yoshimura[2,3,4,5]

[1]Graduate School of Integrated Science and Technology, Shizuoka University, 3-5-1 Johoku, Hamamatsu 432-8561, Japan

[2]Department of International Health and Medical Anthropology, Institute of Tropical Medicine, Nagasaki University, Nagasaki 852-8523, Japan

[3]Department of Biological Science, Tokyo Metropolitan University, Hachioji, Tokyo, 192-0397, Japan

[4]University Museum, the University of Tokyo, Bunkyo-ku, Tokyo, 113-0033, Japan

[5]Marine Biosystems Research Center, Chiba University, Uchiura, Kamogawa, Chiba 299-5502, Japan

Corresponding author before publication: J. Yoshimura (yoshimura.jin@shizuoka.ac.jp)

ORCID: 0000-0003-1610-1386

Corresponding author after publication: T. Okabe (okabe.takuya@shizuoka.ac.jp) ORCID: 0000-0001-7518-5837

Keywords: multiplicative growth, log-normal distribution, bet hedging behavior, adaptive coin-flipping, variable environment

Abstract:

Temporal variations in population size under unpredictable environments are of primary concern in evolutionary ecology, where time scale enters as an important factor while setting up an optimization problem. Thus, short-term optimization with traditional (arithmetic) mean fitness may give a different result from long-term optimization. In the long-term optimization, the concept of geometric mean fitness has been received well by researchers and applied to various problems in ecology and evolution. However, the limit of applicability of geometric mean has not been addressed so far. Here we investigate this problem by analyzing numerically the probability distribution of a random variable obeying stochastic multiplicative growth. According to the law of large number, the expected value (i.e., arithmetic mean) manifests itself as a proper measure of optimization as the number of random processes increases to infinity. We show that the finiteness of this number plays a crucial role in arguing for the relevance of geometric mean. The geometric mean provides a satisfactory picture of the random variation in a long term above a crossover time scale that is determined by this number and the standard deviation of the randomly varying growth rates. We thus derive the applicability condition under which the geometric mean fitness is valid. We explore this condition in some examples of risk spreading behavior.

Keywords: multiplicative growth, stochastic environment, mean fitness, finite-size effect, long-term sustainability

42

1. Introduction

Variation in population size is of central importance in evolutionary biology. Some portion of variation should originate from stochastic or random processes for known or unknown reasons. In optimizing with respect to the stochastic degrees of freedom, time scale may matter importantly, i.e., short-term optimization may not be optimal in a long term. Thus, it is of primary importance to investigate the time-scale dependence of a predicted behavior of the population. In biology of population growth under stochastic environments, it is acknowledged that the use of the expected value, the arithmetic mean, of growth rates (usually called mean fitness, e.g., the number of offspring per female parent) can give an erroneous picture of nearly every population (Dempster 1955; Cohen 1966; Cohen 1968; Lewontin and Cohen 1969; Iwasa and Cohen 1989). Instead, the geometric mean of growth rate (geometric mean fitness) provides a satisfactory picture (Yoshimura and Clark 1991, 1993; Yoshimura and Jansen 1996; Jansen and Yoshimura 1998; Yoshimura et al. 2009; Yoshimura et al. 2013a, b). For example, bet hedging (e.g., risk spreading and adaptive coin-flipping) has been understood in terms of geometric mean fitness (Slatkin 1974; Seger and Brockmann 1987; Philippi and Seger 1989; Cooper and Kaplan 1982; Kaplan and Cooper 1984; Yasui and Yoshimura 2018); see also Iwasa (1991, 2000). From a theoretical perspective, the geometric mean represents the median of growth rates (Okabe and Yoshimura 2020) and the median provides a reasonable solution of the St. Petersburg Paradox in which the expected value does not make sense (Okabe et al. 2019).

Thus, on the one hand, the geometric mean fitness seems valid in explaining bet hedging adaptation. On the other hand, the arithmetic-mean fitness appears valid from a

65 standard theoretical perspective (Fisher 1930; Dobzhansky 1937; Hartl and Clark 1997). If
66 the geometric mean is the valid measure of long-term optimization, it suggests itself that
67 the arithmetic mean has a limited range of validity. Conversely, the geometric mean has a
68 limited range of validity if the arithmetic mean holds good in some cases. (It is our view
69 that geometric mean fitness makes sense only under restricted conditions. Another possible
70 attitude is to have recourse to the geometric mean fitness `principle', according to which
71 optimizing arithmetic and geometric means may align in a short term but do not exclude
72 from each other. We do not take this view as it does not answer but obviates the questions
73 of this study, i.e., when and how the geometric mean comes into play.) As a matter of fact,
74 the theoretical basis of the validity of the geometric mean concept has not been established.
75 It is unknown quantitatively how long it must be for the geometric mean to hold good in the
76 long-term optimization. Thus, a theoretical consideration suggests the presence of a
77 crossover time scale to separate the short term and the long term in which the arithmetic
78 mean and the geometric mean are valid, respectively. It is not a trivial matter why and how
79 the concept of geometric mean fitness manifests itself in the population growth under
80 stochastic conditions. The present study investigates this problem numerically and
81 analytically. It should be remarked that the present problem has nothing to do with a
82 classical problem of polymorphism in a large diploid random mating population, whose
83 condition is conveniently expressed in terms of the arithmetic and geometric mean fitnesses
84 of recessives (but not of dominants) (Haldane and Jayakar 1963). We assume haploid and
85 asexual inheritance for simplicity.

86 The outline of our paper is as follows. The next section (Sec. 2) explains the

theoretical backgrounds of the problem addressed in the present study based on the population growth model with random growth rates. In Sec. 3, we present the numerical as well as analytical results showing a crossover from the arithmetic mean to the geometric mean of the growth behavior of the population size. In the last section, the present results are applied to argue for some representative prior studies founded on the geometric mean fitness (Sec. 4.1, 4.2). Moreover, we discuss the scope of application of the geometric mean in biological evolution, especially on an evolutionary perspective in paleontology (Sec. 4.3).

2. Model and Backgrounds

Consider a population growth model in which number (population size) S_t in the t-th generation grows in a multiplicative manner as

$$S_{t+1} = R_t S_t, \qquad (1.1)$$

where the growth rate R_t is an independently and identically distributed random variable taking a certain value r_n with a given probability p_n ($\sum_n p_n = 1$). We assume that natural selection acts on S_T at the T-th generation to take into account that evolution by natural selection is not necessarily "short-sighted" (i.e., T need not be 1). Thus, the quantity of interest is the growth ratio between the change in T generations, i.e.,

$$S_T/S_0 = R_0 R_1 R_2 \cdots R_{T-1} = \prod_{n=0}^{T-1} R_n. \qquad (1.2)$$

This ratio is not a constant but a random variable obeying a certain probability distribution. However, it is often approximately replaced with a representative constant value, i.e., the T-

th power of the geometric mean of the growth rate r_n (Cohen 1966; Lewontin and Cohen 1969; Yoshimura and Clark 1991; Cohen 1993),

$$S_T/S_0 \simeq \left(m_{\mathrm{geo}}\right)^T, \qquad (1.3)$$

where the geometric mean is given by

$$m_{\mathrm{geo}} = r_a^{p_a} r_b^{p_b} \cdots = \prod_n r_n^{p_n}. \quad (1.4)$$

Intuitively, this approximation is based on the following expectation seemingly valid for a sufficiently large value of T. In the T factors on the right-hand side of Eq. (1.2), each outcome r_n is expected to occur about Tp_n times on average, so that $S_T/S_0 \simeq r_a^{Tp_a} r_b^{Tp_b} \cdots = \left(m_{\mathrm{geo}}\right)^T$ (Cohen 1966). On the other side, we may have recourse to the law of large numbers, i.e., a centuries-old theorem in probability theory. According to this mathematical theorem, the results obtained from a number of trials should get closer to the expected value (i.e., the arithmetic mean, the common type of average), as the number of trials increases to infinity. Thus, there is a good reason for using the common type of average, namely,

$$S_T/S_0 = (m_{\mathrm{arith}})^T, \quad (1.5)$$

with the arithmetic mean

$$m_{\mathrm{arith}} = p_a r_a + p_b r_b + \cdots = \sum_n p_n r_n, \quad (1.6)$$

which is the average (expected value) of each of T factors (R_t) in Eq. (1.2) (Fisher 1930; Dobzhansky 1937; Hartl and Clark 1997). It should be emphasized that Eq. (1.5) is mathematically exact while Eq. (1.3) is not. (In the sense that the larger T is, the better Eq.

(1.5) holds. Both of Eqs. (1.3) and (1.5) are approximate for a finite value of T.) However, Lewontin and Cohen (1969) pointed out that the expected value may give a completely erroneous picture of nearly every population by showing that the population size S_T should vanish in a long term with almost certainty if the geometric mean is less than unity. If we consider the long-term behavior of two populations with different alleles, the population with the higher geometric mean will go to fixation (the other with the lower geometric mean will extinct) almost certainly (Cohen 1993; Bulmer 1994). Thus, the geometric mean fitness provides a long-term measure of fixation or extinction of competing populations. It should be remarked, however, extinction will not come about in the simple model (1.1) alone, because this model usually excludes the possibility of $R_t = 0$ in order not to make the random variable $\log R_t$ unbounded. (The extinction problem in the model allowing for $R_t = 0$ is treated in a straightforward manner (Nii et al (2019).) Thus, it is not trivial how the geometric mean plays an apparently important role in its long-term behavior. Let us note that the model in Eq. (1.1) does not allow us to discuss within-generation correlation, which may have interesting implications for bet-hedging strategies to evolve (Starrfelt and Kokko 2012; Haaland et al. 2019). Bet-hedging strategies are often categorized into between-generation and within-generation strategies, which are often associated with coarse-grained and fine-grained environments, respectively. While the distinction between them may be of biological significance, it has little to do with the main interest of the present study. We are interested in solidifying the basis of the geometric mean concept employed as an appropriate measure of long-term fitness in a coarse-grained environment. While empirical observations may imply validity of this concept, the previous studies have

150 assumed its validity without asking under what conditions its use is justified. In any case,
151 theoretical expectations point to an exponential variation (dependence on T) of S_T. (The
152 logarithm of S_T tends to vary in proportion to T, so that $(\log S_T)/T$ is a good measure of
153 the exponential variation. See Fig.3.) In fact, as noted above, S_t is a random variable
154 distributed over a very wide range (Fig. 1). Each temporal variation of S_t exhibits a
155 uniquely zigzag course, which is determined by actual realizations of the random variable,
156 the growth rate at each step. Accordingly, it can show a steady variation only in very
157 special cases. Sample variations in Fig. 1 are shown by way of illustration, which therefore
158 should not be taken to be representative of possible outcomes. Each sample result may
159 show abrupt changes from time to time, so that the overall behavior of each realization does
160 not necessarily resemble a theoretical (exponential) variation. Our aim here is to show
161 which approximation (Eqs. (1.3) and (1.5)) becomes valid under what conditions.

162 Figure 2 shows the frequency distribution of the population sizes at the 20th
163 generation, $S_{T=20}$, obtained by M = 1,000,000 realizations of numerical simulation. A
164 linear plot in Fig. 2(a) indicates that the distribution has a very long tail (Okabe and
165 Yoshimura 2020). For the parameters used in Fig. 2 (r_1 = 0.5, r_2 = 1.7 and $p_1 = p_2$ = 1/2),
166 the geometric mean growth rate is given by $\left(m_{\mathrm{geo}}\right)^T \simeq 0.197$, which corresponds to the
167 peak of the log-log plot in Fig. 2(b). This is mathematically shown as follows. The central
168 limit theorem states that, as T increases, $\log(S_T/S_0) = \sum_{t=0}^{T-1} \log r_t$ converges to the normal
169 distribution with mean μT and variance $\sigma^2 T$, where μ and σ^2 are the mean and variance of
170 $\log r_t$, i.e.,

171 $$\mu = \sum_n p_n \log r_n \qquad (1.7)$$

172 and

173 $$\sigma^2 = \sum_n p_n (\log r_n - \mu)^2. \qquad (1.8)$$

174 Accordingly, S_T obeys the log-normal distribution with its mean at $e^{\mu T}$. Since $m_{\mathrm{geo}} = e^{\mu}$,
175 it is concluded that $\log S_T$ is peaked at $S_T = \left(m_{\mathrm{geo}}\right)^T$, i.e., 0.197 for $r_1 = 0.5$, $r_2 = 1.7$ and
176 $p_1 = p_2 = 1/2$ in Fig. 2. To sum up, the geometric mean m_{geo} manifests itself in the
177 probability distribution of $\log(S_T/S_0)$, while the expected value m_{arith} does in that of
178 S_T/S_0. We underline the importance of distinguishing two random variables, S_T/S_0 and its
179 logarithm $\log(S_T/S_0)$ (Fig. 2). On the one hand, the latter ($\log(S_T/S_0)$) is directly related to
180 the geometric mean m_{geo} (Yoshimura et al. 2009). On the other hand, the quantity of our
181 interest is the former (S_T/S_0). It is not trivial why and how the geometric mean $\left(m_{\mathrm{geo}}\right)^T$
182 comes into play in discussing the population size S_T/S_0. It even appears doubtful if the peak
183 of the logarithm of population size has any real (e.g., biological) significance. The present
184 study aims at filling the logical gap of using the geometric mean for evaluating the
185 expected outcome of S_T without introducing the logarithmic variable ($\log(S_T/S_0)$).

186

187 **3. Analysis and Results**

188 The point we make is based on the observation that the distribution of S_T/S_0 after a long
189 time T gets so long tailed that extremely large values are practically negligible owing to
190 their extremely low probability of occurrence (i.e., ($\mathrm{Prob}(S_T/S_0 > K)$ becomes negligible

for a large value of K). The population after T generations, S_T, is obtained from the initial size $S_0 = 1$ by multiplying a total number T of randomly varying growth rates, R_i (Eq. (1.2)). If we perform a total of (hypothetical) M simulations, we obtain M results for the final size S_T. To achieve a continuous distribution, the number M must be infinitely large, which is not possible in numerical analysis. As a sufficiently large value, we took M = 1,000,000, which makes Fig. 2(b) resemble a bell curve. Moreover, in practice, we must consider that the number of realizations in nature (real simulations), N, is finite. In natural selection in the wild, the number of natural processes may be large but cannot be mathematical infinity ($N \ll \infty$). Since the frequency distribution of S_T is very long tailed (Fig. 2), extreme (tail) values are very unlikely to be realized in practice. To express it mathematically, let us denote the n-th biggest result of the M results as $S_{\max}(n/M)$. The probability of occurrence of a tail value $S_T > S_{\max}(n/M)$ is n/M. This probability is $1/N$ if we select n and M such that $n/M = 1/N$. Thus, in practice, tail values $S_T > S_{\max}(n/M)$ for $n/M = 1/N$ are considered unlikely events when the total number N is large but finite. Note that the threshold size $S_{\max}$ is determined by N if M is sufficiently large. In fact, it increases steadily as N increases. In Figure 2, the threshold values $S_{\max}$ for N = 10, 100 and 1000 are indicated with vertical lines. The dashed lines with N =100 correspond to the n=10,000th biggest result of the M=1,000,000 simulations. Roughly speaking, this value ($S_{\max} \simeq 50$) corresponds to the 100th biggest result in the total of 10,000 simulations, the 10th biggest result in 1,000 simulations, and similarly the 1st biggest result in 100 simulations. Accordingly, we expect that tail values S_T larger than this value are unlikely to be realized if the total number of simulations is as small as N=100.

To take it into account that sample size N is finite, we consider the conditional expectation value in which large tail values $S_T > S_{\max}$ are omitted from consideration. Consequently, we aim at providing an answer to the problems remarked in the introduction, i.e., the theoretical basis on the relevance of the geometric mean concept and its range of validity. In this approach, we follow and quantify the argument of Lewontin and Cohen (1969), in which more emphasis is put on the probability of occurrence of stochastic processes than on their average over all possible outcomes. It is noted that $S_{\max}$ depends on N as mentioned above (Fig. 2). Mathematically, the conditional expectation is given by

$$\langle S_T \rangle_N = E[S_T | S_T \leq S_{\max}]. \quad (2.1)$$

It is expected that this conditional expectation expresses biological reality more properly than the ideal mathematical expectation calculated for the hypothetical infinite samples. Numerical evaluation shows that $\langle S_T \rangle_N$ varies approximately exponentially depending on generation (time) T. Accordingly, it is convenient to focus on the 'growth rate' $\log[\langle S_t \rangle_N] / t$ (the logarithm of the average, not to be confused with the average of the logarithm $\langle \log S_t \rangle / t$). Here, the logarithm is taken just for the sake of presentation. Figure 3 shows the t-dependence of $\log[\langle S_t \rangle_N] / t$ for $N = 10$, 100 and 1000, where the horizontal axis (generation t) is plotted with a logarithmic scale. The numerical results indicate that the growth rate $\log[\langle S_t \rangle_N] / t$ gradually shifts from the logarithm of the arithmetic mean value m_{arith} to that of the geometric mean value m_{geo} as generation (time) t increases. It is remembered that these means m_{arith} and m_{geo} are given by Eqs. (1.6) and (1.4), respectively, in terms of the stochastic growth rates of the multiplicative model in Eq. (1.1).

The larger N, the slower the approach to m_{geo}. Thus, the geometric-mean growth ratio provides a good approximation in a long term, especially for a not too large sample size N. It is important to remark that the approach to m_{geo} is due to N being finite (not infinite). While we assume that the environment fluctuates randomly between two possible states in Figs. 1-3, the above result on m_{geo} does not depend on this assumption (Appendix).

The above results indicate that the geometric mean m_{geo} is an appropriate measure beyond a certain crossover scale t_{cr}, i.e., for generation $t \gg t_{\mathrm{cr}}$. This scale should increase as the sample size N increases. Indeed, an analytical expression for t_{cr} is obtained as follows. According to the central limit theorem, the probability distribution of $\log S_t = \log S_0 + \sum_t \log R_t$ converges to the normal distribution with mean μt and variance σt, where

$$\mu = \sum_n p_n \log r_n \qquad (2.2)$$

and

$$\sigma^2 = \sum_n p_n (\log r_n - \mu)^2, \qquad (2.3)$$

are the mean and variance of the random variable $\log R_n$ (Lewontin and Cohen 1969). Accordingly, S_t obeys the log-normal distribution with its μ and σ^2 parameters as given by the last two equations. Using an approximation for the log-normal distribution, we obtain

$$t_{\mathrm{cr}} = (C(N)/\sigma)^2, \qquad (2.4)$$

where $C(N) = \Phi^{-1}(1 - 1/N)$ with Φ^{-1} being the inverse of the cumulative distribution function (cdf) of the standard normal distribution (Appendix).

In Fig. 4(a), this crossover scale t_{cr} is plotted against the sample size N. For

example, we have $t_{\mathrm{cr}} \simeq 26$ for $N = 1000$ (cf. Fig. 3). The scale t_{cr} increases with the sample size N. Accordingly, it diverges in the mathematical limit of infinite size $N \to \infty$, where the geometric mean m_{geo} ceases to be relevant while the arithmetic mean m_{arith} holds good. Note that the geometric (arithmetic) mean becomes approximately valid for $t \gg t_{\mathrm{cr}}$ ($t \ll t_{\mathrm{cr}}$). Similarly, the traditional arithmetic mean m_{arith} holds good ($t_{\mathrm{cr}} \to \infty$) when there is no variation ($\sigma = 0$) in the population growth (Eq. (2.3)). The main result is schematically shown in Fig. 4(b).

4. Applications and Discussions

4.1 Adaptive coin-flipping

Consider the ptarmigan adopting white or dark coloration as a prototypical example of adaptive coin-flipping (Cooper and Kaplan 1982). If one chooses white, it will be well camouflaged in case the winter ground is snow-covered but will be conspicuous if there is no snow. Conversely, the dark coloration will be advantageous if the winter is snowless but disadvantageous if it is not. Assume that snowy and snowless winters occur randomly with equal frequency, and moreover that the population will double in size in each season if its members are cryptically colored but shrink to 40% of its former size if the coloration is conspicuous. The geometric mean fitness of pure strategies (whether white or dark) is $2^{0.5} \times 0.4^{0.5} = 0.89$, which (being less than one) signifies that either is not maintained in the long run. On the other hand, the mixed strategy where each individual randomly chooses white or dark by "flipping a coin" gives $1.2^{0.5} \times 1.2^{0.5} = 1.2$. Thus, the latter "gambling" genotype

is substantially fitter than either of its deterministic competitors (Cooper and Kaplan 1982). In this case, the coin-flipping strategy gives no difference between the geometric and arithmetic mean fitnesses ($1.2^{0.5} \times 1.2^{0.5} = 1.2 = 0.5\times 1.2 + 0.5\times 1.2$). Accordingly, we should assess the significance of the geometric mean in pure strategies. Note that the advantage of the coin-flipping strategy cannot be explained by using the arithmetic mean fitness (pure white strategy gives: $0.5\times 2 + 0.5\times 0.4 = 1.2$; pure dark strategy gives: $0.5\times 0.4 + 0.5\times 2 = 1.2$).

According to the present results (Fig. 4(a)), since $\sigma = 0.80$ from Eq. (2.3), we obtain $t_{cr} = 18$ and 31 generations for $N = 100$ and 1000, respectively. This means that we find the crossover point is the 18th generation for sample size of 100. If we consider fewer generations, the usual arithmetic mean fitness is a sound, valid measure. In contrast, if we consider more generations, we better use the geometric mean fitness. These 18 (31) generations for the sample size of 100 (1000) are not so unrealistically large as to invalidate the use of the geometric mean. Thus, Cooper and Kaplan (1982) is valid in arguing for the adaptation of the coin-flipping strategy. Various cases of adaptive coin-flipping are also discussed (Kaplan and Cooper 1984).

4.2 Risk-spreading behavior

The next example is risk-spreading behavior of the cabbage butterfly (*Pieris rapae*) (Yoshimura and Jansen 1996; Jansen and Yoshimura 1998). Suppose a female butterfly distributing its offspring (eggs) over two types of habitat with different qualities. One

habitat, say habitat 1, is highly productive but suffers from occasional catastrophes in which only very few offspring survive, while the other habitat is constant in quality but the quality is low so that a population that uses this habitat only is doomed to extinction. An individual produces total m offspring, of which a fraction f is deposited in habitat 1. In habitat 1, the survivorship of offspring takes values S_a ($< 1/m$) with probability p and S_b ($> 1/m$) with probability $1 - p$, where p is the probability of a catastrophe to occur. In habitat 2, it is S_c ($< 1/m$) with certainty. The optimal fraction f^* is obtained by maximizing the geometric mean of the growth rates $G(f) = m(fS_a + (1 - f)S_c)^p(fS_b + (1 - f)S_c)^{1-p}$. Specifically, we obtain $f^* = 0.617$ and $G(f^*) = 1.45$ for $mS_a = 0.005$, $mS_b = 5$, $mS_c = 0.7$ and $p = 1/3$ (Fig. 2 of Jansen and Yoshimura (1998)).

In this example, we obtain $\mu = 0.37$ and $\sigma = 1.2$ from Eqs. (2.3) and (2.4). For this large value of σ, the critical generation t_{cr} in Eq. (2.4) is sufficiently small to guarantee the use of the geometric mean $G(f)$ without any severe restriction to the generation number t (e.g., $t_{cr} = 3$, 4 and 5 for $N = 50$, 110 and 250, respectively). This example shows that the geometric mean fitness becomes a reliable measure in the presence of a strong variation in the growth rates (a large value of σ), where the population is susceptible to extinction.

4.3 General discussions

The geometric mean growth rate provides a good picture of long-term behavior. The present study indicates that this is approximately true beyond a crossover time scale t_{cr} determined by sample size N. The crossover scale increases without limit as N increases.

317 However, the N dependence of t_{cr} is so weak that it is rather practical to consider that t_{cr} is
318 moderately finite, i.e., not exceeding hundreds (Fig. 4a). Note that the x-axis of Fig. 4a is
319 logarithmic, so that the N dependence of t_{cr} is logarithmically weak. It is admittedly a
320 difficult problem to evaluate N practically. However, a rough guess may be made by noting
321 that its inverse $1/N$ is related to the accuracy of observation data. The accuracy in
322 ecological systems should be some orders of magnitudes less than in physical systems,
323 where an accuracy of several orders of magnitude is not rare. Accordingly, it is not
324 practical to assume N as large as a million in ecological systems. The scale depends also on
325 the variation σ^2 of random growth rates. The larger σ^2, the smaller t_{cr}. Accordingly, the
326 geometric mean picture holds good when the random variation in the growth rate is strong
327 (Fig. 4). Especially, a population on the verge of extinction may have a strong variation of
328 the growth rate. The emerging picture of the present study is shown in Fig. 4b, which
329 illustrates the applicability regimes of arithmetic and geometric means. It is remarked that a
330 similar figure is presented in a different context (Haaland et al. 2019).

331 In biological evolution, it is important to remember that we are concerned with a
332 finite number of temporal sequences of events. In mathematical treatment of random
333 events, it is almost always implicitly assumed that the statistical average over all
334 theoretically possible outcomes represents a typical outcome. However, there can be many
335 real-life situations in which this assumption may not hold good. This remark holds
336 particularly in such a situation as the present model describes, where theoretically possible
337 outcomes of a stochastic population dynamics diverge away from each other in an
338 exponential manner. Consequently, the statistical mean over observed events is strongly

affected by whether some extremely unlikely events occur actually. In practice, e.g., the events of probability 0.0001 may be ignored when we survey 100 trials at most. This is the basic idea of our approach, in which a crossover timescale manifests itself owing to the temporal diversification of random outcomes.

The present study shows that it is not true that the geometric mean concept of wide use in various fields is valid without reservation or qualification. There is a time window within which this concept serves as a convenient and approximate, if not mathematically exact, measure of long-term optimization. The time window depends on the number of trials, and so on the situation. Therefore, the limit of applicability of the geometric-mean growth rate is not determined solely by the mathematical details of the random process but it also depends on the actual situation usually not considered in a mathematical model. At an extreme end lies the view of history as contingency, where any past event is singular (occurred only once in the past) (Gould 1989, 2002). At the opposite end lies the recurrence view of history that assumes the mathematical ideality of an infinite number of similar repeated events. The latter recurrence view enables us to predict the evolutionary direction in life (Vermeij 2004, 2006). The actuality lies in between the two extremes. The actual problem can be practically akin more to a singular (one-time) event than to the mathematical limit of infinite repetitions, so that the geometric mean fitness becomes more appropriate than the arithmetic mean fitness in discussing the evolutionary history of life.

The above argument may explain why the view of biological evolution is so different between biologists and paleontologists (Simons 2002). The punctuated equilibria in the geological time scale may be more appropriately considered under the geometric

mean fitness (Eldredge and Gould 1972; Gould and Eldredge 1977), while the gradual evolution of genetic traits in population genetics is under the arithmetic mean fitness (Fisher 1930; Dobzhansky 1937; Hartl and Clark 1997). Thus, both views of evolution are complementary and valid in its own domain of applications. It is an interesting future research direction to study if the finiteness of actual trials has an observable effect on the evolution of a biological system, or more generally on evolving complex systems.

Appendix

In the long-time limit $t \to \infty$, S_t obeys the log-normal distribution with its μ and σ^2 parameters as given in the main text. In the log-normal distribution, the probability that S_t is less than K is given by $\mathrm{Prob}(S_t < K) = \mathrm{Prob}\left(\frac{1}{t}\sum_{\mathrm{t}=0}^{\mathrm{t}-1} \log r_t < \frac{1}{t}\log K\right) = \Phi\left(\frac{\log K - \mu t}{\sigma\sqrt{t}}\right)$, where $\Phi(y)$ is the cumulative distribution function (cdf) of the normal distribution with mean 0 and standard deviation 1. Owing to $\mathrm{Prob}(S_t > S_{\max}) = 1/N$, or $\mathrm{Prob}(S_t < S_{\max}) = 1 - \frac{1}{N}$, we obtain $S_{\max} = e^{\mu t + C(N)\sigma\sqrt{t}}$, where $C(N) = \Phi^{-1}\left(1 - \frac{1}{N}\right)$. On the other side, the conditional expectation is also expressed as $E[S_t | S_t < K] = e^{\mu t + \frac{\sigma^2}{2}t}\Phi\left(\frac{\log K - \mu t - \sigma^2 t}{\sigma\sqrt{t}}\right)/\Phi\left(\frac{\log K - \mu t}{\sigma\sqrt{t}}\right) = e^{\mu t + \frac{\sigma^2}{2}t}\Phi\left(C(N) - \sigma\sqrt{t}\,\right)/(1 - \frac{1}{N})$, where we substituted $K = S_{\max}$ in the second equation. For a sufficiently large t, we may use an asymptotic formula $\Phi(x) \simeq e^{-\frac{x^2}{2}}/(|x|\sqrt{2\pi})$ valid for $x \to \pm\infty$. Consequently, we obtain $E[S_t | S_t < S_{\max}] \simeq e^{\mu t}/(\sqrt{2\pi t}\sigma)$, for $\sigma\sqrt{t} \gg C(N)$, or for $t \gg t_{\mathrm{cr}}$ with $t_{\mathrm{cr}} = (C(N)/\sigma)^2$. Noting that $e^{\mu} = m_{\mathrm{geo}}$ by Eqs. (1.2) and (2.2), we obtain $\langle S_t \rangle_N \sim \left(m_{\mathrm{geo}}\right)^t$ for $t \gg t_{\mathrm{cr}}$.

Data Accessibility. This article has no additional data

Code availability. This article has no custom code essential to the results.

Authors Contributions. TO conceived and performed the study. TO and JY wrote the manuscript.

Conflicts of interest/Competing Interests. We declare we have no competing interests.

Funding. This work was partly supported by grants-in-aid from the Japan Society for Promotion of Science (no. 21K12047 to TO and nos. 22255004, 22370010, 26257405, 15H04420 to JY)

391 **References**

392 Bulmer M (1996) Theoretical Evolutionary Ecology, Sinauer Associates Publishers.

393 Cohen D (1966) Optimizing reproduction in a randomly varying environment. Journal of
394 Theoretical Biology 12: 119-29.

395 Cohen D (1968) A general model of optimal reproduction in a randomly varying
396 environment. Journal of Ecology 56: 219-228.

397 Cohen D (1993) Fitness in Random Environments. In Yoshimura J, Clark CW. eds.,
398 Adaptation In Stochastic Environments. Lecture Notes in Biomathematics Volume 98,
399 Springer-Verlag, Berlin (pp 8-25).

400 Cooper WS, Kaplan RH (1982) Adaptive Coin-Flipping: A Decision Theo retic
401 Examination of Natural Selection for Random Individual Variation, Journal of Theoretical
402 Biology 94: 135-151.

403 Dempster ER (1955) Maintenance of genetic heterogeneity. Cold Spring Harbor
404 Symposium in Quantitative Biology 20: 25-32.

405 Dobzhansky, Th (1937) Genetics and the Origin of Species. Columbia University Press,
406 New York. (2nd ed., 1941; 3rd ed., 1951)

407 Eldredge N, Gould SJ (1972) Punctuated equilibria: an alternative to phyletic gradualism.
408 In T.J.M. Schopf, ed., Models in Paleobiology. San Francisco: Freeman Cooper. pp. 82-
409 115.

410 Fisher, RA (1930) The Genetical Theory of Natural Selection, Clarendon Press, Oxford.

411 Gould SJ (1989) Wonderful Life: The Burgess Shale and the Nature of History (Norton,
412 New York).

413 Gould SJ (2002) The Structure of Evolutionary Theory (Belknap, Cambridge, U.K.).

414 Gould SJ, Eldredge N (1977) Punctuated equilibria: the tempo and mode of evolution
415 reconsidered. Paleobiology 3 (2): 115-151.

416 Haaland TR, Wright J, Ratikainen II (2019) Bet-hedging across generations can affect the
417 evolution of variance-sensitive strategies within generations. Proc R Soc B Biol Sci 286.

418 Haldane JBS, Jayakar SD (1963) Polymorphism due to selection of varying direction.
419 Journal of Genetics 58: 237-242.

420 Hartl D, Clark A (1997) Principles of Population Genetics, 3rd edition. Sinauer, 1997.

421 Iwasa Y, Cohen D (1989) Optimal growth schedule of a perennial plant. American
422 Naturalist 133:480-505.

423 Iwasa Y (1991) Pessimistic plants: the optimal growth schedule in fluctuating
424 environments. Theoretical Population Biology 40:246-268.

425 Iwasa Y (2000) Dynamic optimization of plant growth. Evolutionary Ecology Research 2:
426 437-455.

427 Jansen VAA, Yoshimura J (1998) Population can persist in an environment consisting of
428 sinks only. Proceedings of the National Academy of Sciences 95: 3696-3698.

429 Kaplan RH, Cooper WS (1984) The Evolution of Developmental Plasticity in Reproductive
430 Characteristics: An Application of the "Adaptive Coin-Flipping" Principle, The American

431 Naturalist 123: 393-410.

432 Lewontin RC, Cohen D (1969) On population growth in a randomly varying environment.
433 Proceedings of the National Academy of Sciences, USA 62: 1056-1060.

434 Nii M, Okabe T, Ito H, Morita S, Yasuda Y, Yoshimura J (2019) Bankruptcy is an
435 inevitable fate of repeated investments with leverage. Scientific Reports 9: 13745.

436 Okabe T, Nii M, Yoshimura J (2019) The median-based resolution of the St. Petersburg
437 paradox. Phys Lett A 383: 125838.

438 Okabe T, Yoshimura J (2020) A new median-based formula for the Black-Scholes-Merton
439 Theory. Physica A (to appear).

440 Okabe T, Yoshimura J (2020) Practical implications of the generalized central limit
441 theorem (submitted).

442 Philippi T, Seger J (1989) Hedging one's evolutionary bets, revisited. Trends Ecol Evol 4:
443 41–44.

444 Seger J, Brockmann HJ (1987) What is bet-hedging? In Oxford surveys in evolutionary
445 biology, vol. 4 (eds, Harvey P. H.& Partridge L.), pp. 182–211. Oxford, UK: Oxford
446 University Press.

447 Simons AM (2002) The continuity of microevolution and macroevolution. J Evol Biol 15:
448 688-701.

449 Slatkin M (1974) Hedging one’s evolutionary bets. Nature 250: 704-705.

450 Starrfelt J, Kokko H (2012) Bet-hedging - a triple trade-off between means, variances and

451 correlations. Biol Rev 87:742-755.

452 Vermeij GJ (2004) Nature: An Economic History (Princeton Univ. Press, Princeton).

453 Vermeij GJ (2006) Historical contingency and the purported uniqueness of evolutionary
454 innovations. Proceedings of the National Academy of Sciences 103 (6) 1804-1809; DOI:
455 10.1073/pnas.0508724103

456 Yasui Y, Yoshimura J (2018) Bet-hedging against male-caused reproductive failures may
457 explain ubiquitous cuckoldry in female birds. Journal of Theoretical Biology 437: 214-221.

458 Yoshimura J, Clark CW (1991) Individual adaptations in stochastic environments
459 Evolutionary Ecology 5: 173-192.

460 Yoshimura J, Clark CW. eds. (1993) Adaptation In Stochastic Environments. Lecture Notes
461 in Biomathematics Volume 98, Springer-Verlag, Berlin (pp193).

462 Yoshimura J, Ito H, Miller III DG, Tainaka K (2013a) Dynamic decision-making in
463 uncertain environments I. The principle of dynamic utility. Journal of Ethology 31: 101-
464 105.

465 Yoshimura J, Ito H, Miller III DG, Tainaka K (2013b) Dynamic decision-making in
466 uncertain environments II. Allais paradox in human behavior. Journal of Ethology 31: 107-
467 113.

468 Yoshimura J, Jansen VAA (1996) Evolution and population dynamics in stochastic
469 environments. Researches on Population Ecology 38: 165-182.

470 Yoshimura J, Tanaka Y, Togashi T, Iwata S, Tainaka K (2009) Mathematical equivalence

471 of geometric mean fitness with probabilistic optimization under environmental uncertainty.
472 Ecological Modelling 220: 2611-2617.
473

Figures

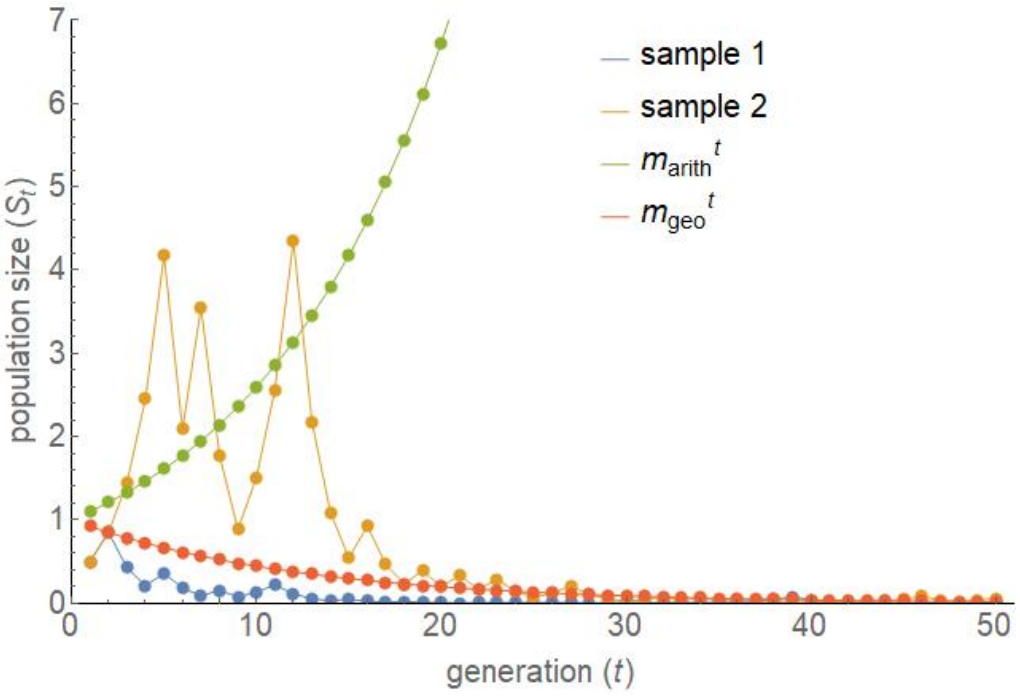

Figure 1. Sample variations of population size S_t. Starting from initial size S_0=1, size S_t of sample 1 shows a steady decrease with little fluctuations, while sample 2 shows large fluctuations before settling to a decrease. Additionally, two smooth curves are theoretical, exponential variations $(m_{\text{arith}})^t$ and $\left(m_{\text{geo}}\right)^t$, where m_{arith} and m_{geo} are the arithmetic mean and the geometric mean, respectively, of the growth ratio (r_i) that varies randomly with given probability (p_i) (r_1=0.5, r_2=1.7, p_1=p_2=1/2).

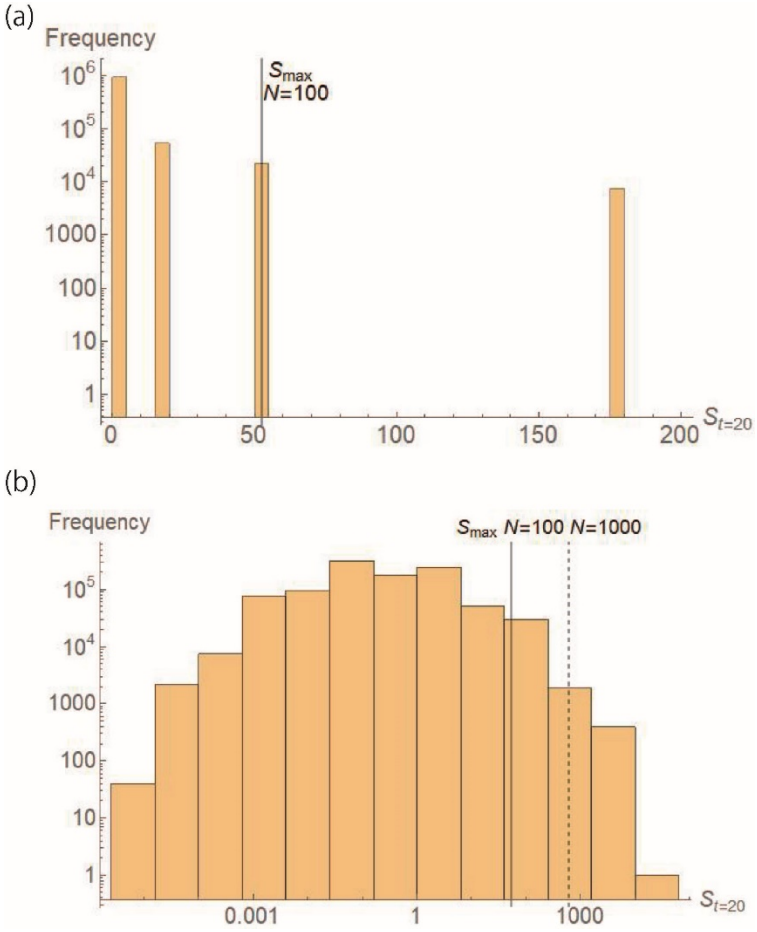

Figure 2. Frequency distribution of population size S_t. The results $S_{t=20}$ at t=20 are obtained by a total of $M = 10^6$ simulations. For later use we show vertical lines indicating $S_{\max}$ for N=100 and 1000 (see Sec. 3). (a) A linear-log plot. (b) A log-log plot. The same data are plotted differently in (a) and (b). In (a), large data $S_{t=20}>200$ on the x-axis are omitted for the purpose of illustration, while they are included in (b). In the limit of an infinite M, the plot in (b) is unimodal with its peak at the geometric mean ($\left(m_{\mathrm{geo}}\right)^{t=20} \simeq 0.197$). ($r_1$ = 0.5, r_2 = 1.7, $p_1 = p_2$ = 1/2).

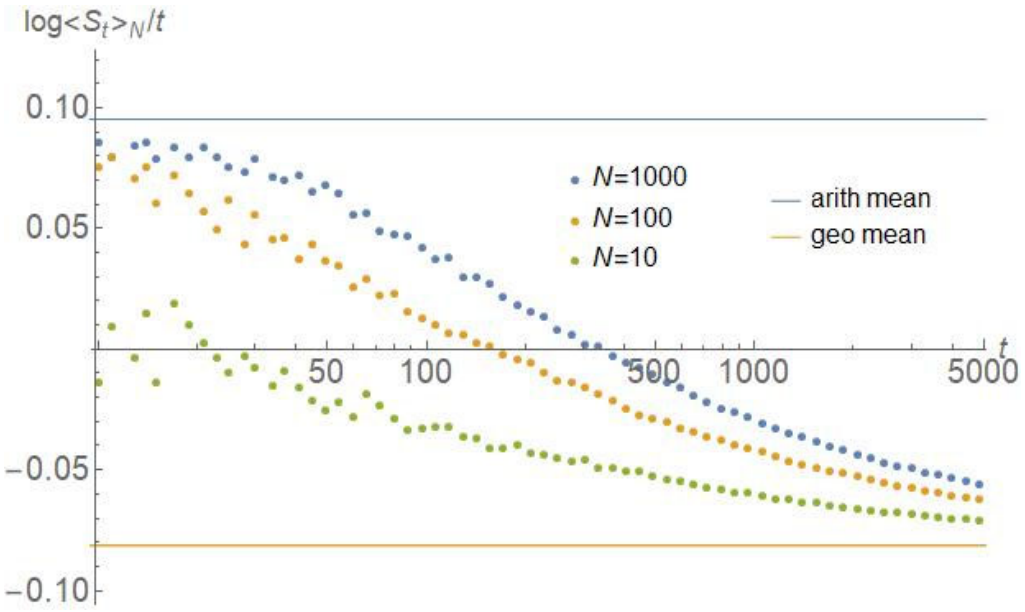

Figure 3. Sample size (N) dependence of the conditional expectation $\langle S_t \rangle_N$. The logarithm of $\langle S_t \rangle_N$ divided by t is shown against t. Two horizontal lines represent the logarithms of the arithmetic mean (upper line) and the geometric mean (lower line). ($M = 10^6$, $r_1 = 0.5$, $r_2 = 1.7$, $p_1 = p_2 = 1/2$).

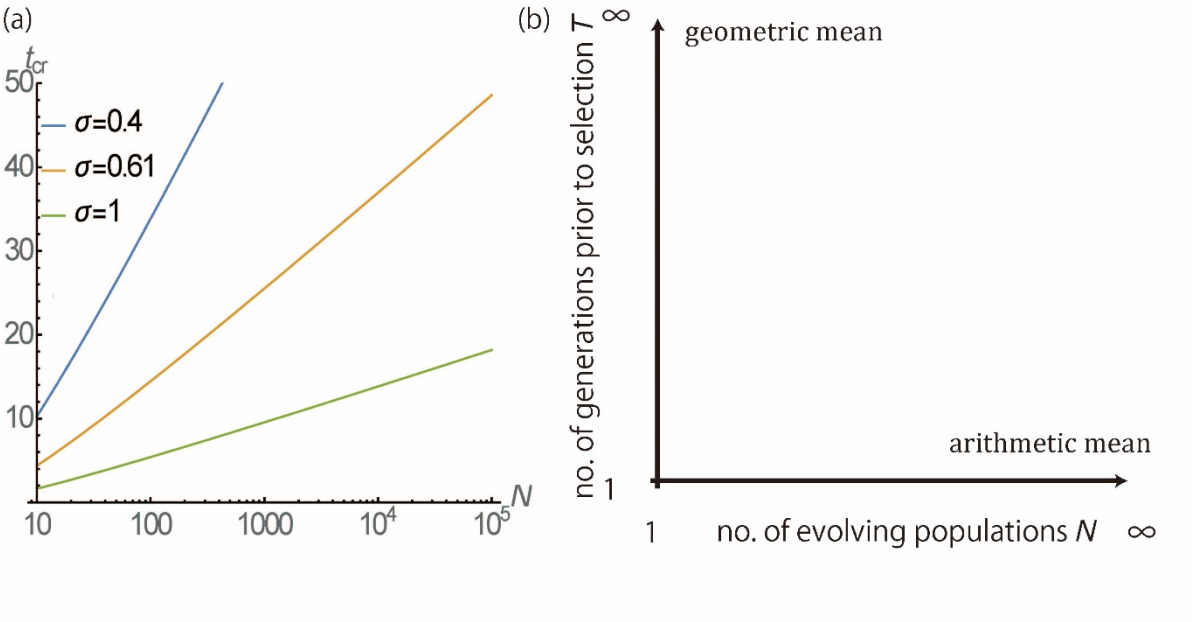

Figure 4. The crossover scales t_{cr} and N_{cr}. (a) The crossover generation number t_{cr} is plotted against sample size N. The geometric-mean growth rate becomes valid when the generation number t is significantly larger than t_{cr}. The middle line for σ =0.61 corresponds to the parameters $r_1 = 0.5$, $r_2 = 1.7$ and $p_1 = p_2 = 1/2$ in Figs. 2 and 3, while two other results for σ = 0.4 and 1 are shown for comparison. Here, σ is the standard deviation of the logarithmic growth rate. (b) Schematic illustration of the main result. A similar figure is presented in a different context (Haaland et al. 2019).